First-principles calculation of oxygen adsorption on Zr(0001) surface: Possible site occupation between the second and the third layer

Masahiro Yamamoto

Institute of Advanced Energy, Kyoto University, Uji, Kyoto 611, Japan
and Ames Laboratory, United States Department of Energy, Department of Physics and Astronomy, Iowa State University, Ames, Iowa 50011

C. T. Chan

Physics Department, Hong Kong University of Science and Technology, Clear Water Bay, Hong Kong
and Ames Laboratory, United States Department of Energy, Department of Physics and Astronomy, Iowa State University, Ames, Iowa 50011

K. M. Ho

Ames Laboratory, United States Department of Energy, Department of Physics and Astronomy, Iowa State University, Ames, Iowa 50011

Shizuo Naito

Institute of Advanced Energy, Kyoto University, Uji, Kyoto 611, Japan
(Received 31 May 1996)

The oxygen adsorption on the Zr(0001) surface is studied using first-principles total-energy and force calculations. We calculated the atomic structure, heat of adsorption, work function, and electronic structure for oxygen occupying various surface and subsurface sites for both the Zr(0001)-(1×1)-O and Zr(0001)-(2×1)-O system. We found that the energetically most favorable occupation sites for oxygen are the octahedral sites between the second and the third layer. The change in the work function induced by oxygen adsorption depends strongly on the position of the adsorbed oxygen atoms and the calculated change of work function at the energetically most favorable site is consistent with previous experiments. A large difference in the electronic structure between the overlayer and subsurface adsorption is also found. [S0163-1829(96)06743-4]

I. INTRODUCTION

Zirconium and its alloys are widely used in the nuclear industry because of its low neutron absorption cross section, excellent corrosion resistance, and high temperature stability. The oxide film that coats the Zr alloys is very stable and effective in preventing the penetration of gases. The study of the initial oxidation of the Zr surface is thus of academic as well as industrial interest.

It is generally believed that dissociative adsorption of light element gases such as hydrogen, nitrogen, and oxygen takes place on transition metal surfaces, and adatoms are chemisorbed at the adsorption sites above the metal surface. This is due to the fact that the binding of the adatom onto the surface is usually more stable than the subsurface or bulk sites. There are, however, exceptions. In the group IV transition metal–light element surface systems such as Ti(0001)-(1×1)-N,[1] Ti(0001)-(2×2)-O,[2–4] Zr(0001)-(2×2)-O,[5–7] Zr(0001)-(2×1)-O,[8,9] Zr(0001)-(1×1)-O,[10] Zr(0001)-(1×1)-N,[11] Zr(0001)-(1×1)-C,[12] and Zr(10$\bar{1}$0)-(2×4)-O,[13] the favorable adsorption sites have been reported to be subsurface, based on low energy electron diffraction (LEED), Auger, and work-function measurements. The unusual adsorption energetics make these systems particularly worth studying from a theoretical point of view. For most of the subsurface chemisorption systems, adsorption sites are found to be (or assumed to be) between the first and second layer of the host. We will see that the O/Zr(0001) system actually favors adsorption sites between the second and the third layer, if the oxygen atoms are confined to sites between two Zr layers.

The zirconium (0001)-oxygen system has been extensively studied by two groups.[5–10,13–16] In this system, a (2×2) LEED pattern was observed at 0.5 monolayer (ML) and a (1×1) LEED pattern was observed at 1 ML. Results from the LEED structure analysis favor subsurface adsorption models, but the details of the structure are still under investigation.[14] For the (2×2) structure at 0.5 ML oxygen coverage, Zhang *et al.* proposed a subsurface three domain model, with three 120° rotated domains of (2×1) oxygen occupying octahedral sites between the top and the second Zr layer.[8] Recently, using tensor LEED analysis, Wang *et al.* proposed a (2×2) array model, with 0.25 ML of oxygen at the octahedral sites between the first and second metal layer and another 0.25 ML between the second and third layer.[15] These two arrays are displaced laterally from one another by a unit translational vector of the Zr(0001) substrate.[15] For the (1×1) structure, Mitchell *et al.* also proposed a subsurface adsorption model, but it was not possible for them to distinguish convincingly between the models involving a single oxygen layer below the zirconium surface and those with oxygen incorporated several layers deep.[10] Recently they

proposed that 0.5 ML of oxygen adatoms are distributed statistically over the octahedral sites between the second and the third metal layer and another 0.5 ML similarly distributed between the first and second layer.[16]

On the theoretical side, no first-principles total energy calculation has been reported for the subsurface adsorption of O/Zr(0001) systems, although the electronic structure of the Ti(0001)-(1×1)-N underlayer adsorption system has been calculated to compare with the photoemission experiments.[17–19] In the present study, the energetics of oxygen adsorption at various sites for the Zr(0001)-(1×1)-O and Zr(0001)-(2×1)-O systems in the single layer model have been investigated by a first-principles total energy and force calculation. The method has been shown to give an accurate description of the structures of solid and solid surfaces.[20,21]

II. FIRST-PRINCIPLES TOTAL-ENERGY AND FORCE CALCULATIONS

The first-principles calculations have been carried out using a pseudopotential method with the local density approximation (LDA).[22] The Hedin-Lundqvist form of exchange-correlation functionals has been used.[23] The Bloch wave functions are expanded in a mixed basis of plane waves and numerical localized wave functions centered on atomic sites.[24] We have used cutoff radii of 2.6 and 1.3 a.u. for the local orbitals of zirconium and oxygen, respectively, and a plane wave basis with kinetic energy up to 20 Ry. The calculated physical properties of the zirconium dioxide in the cubic, tetragonal, and monoclinic phase are in good agreement with experiments.[25]

The surface system in the single layer adsorption model is represented by a supercell with repeated slabs of eight and ten Zr(0001) layers for the (2×1)-O and (1×1)-O systems, respectively, and two oxygen layers on both sides of the slab. The vacuum region between the two slabs has a thickness corresponding to five metal layers. The surface relaxation and the work function calculated for the clean Zr(0001) surface with these slab geometries are in good agreement with experiments.[20] By choosing the origin at the octahedral site at the center of the slab, there are 12 symmetry operations for the (1×1)-O, and four symmetry operations (inversion, mirror, inversion+mirror, identity) for the (2×1)-O system. We used six special **k** points and eight **k** points in the two-dimensional irreducible Brillouin zone to carry out the summation over **k** space for the (1×1)-O and (2×1)-O systems, respectively.

All the interlayer distances for the (1×1)-O system and the interatomic distances in the lateral direction on the mirror plane for the (2×1)-O system are fully relaxed using forces calculated via the Hellmann-Feynman theorem.[26] The initial input potentials are predicted and the acceleration of the force convergence with respect to self-consistency are implemented basing on the recently proposed scheme.[27]

III. RESULTS AND DISCUSSION

A. Energetics

In Figs. 1(a) and 1(b), the various oxygen adsorption sites considered in our calculations are shown schematically for both the (1×1) and (2×1) systems. We will use the symbol O(xy) to denote oxygen atoms at the octahedral site between the xth and the yth metal layer; whereas $T[xy:a$ (or b)$z]$ means the oxygen atoms at the tetrahedral site located directly above (or below) the zth metal layer and between the xth and the yth metal layer. In Fig. 2, the calculated oxygen binding energies for these adsorption sites are shown. The binding energy E_b is defined by

$$E_b(\Theta) = [E_{total}^{slab}(\Theta) - E_{total}^{Zr\ slab}]/N_{oxygen} - E_{total}^{oxygen\ atom}. \quad (1)$$

Here Θ is the coverage defined by the ratio of the number of oxygen atoms N_{oxygen} to the number of zirconium surface atoms $N_{Zr}^{surface}$ in the unit cell. $E_{total}^{slab}(\Theta)$ is the total energy per unit cell of the oxygen adsorbed slab, $E_{total}^{Zr\ slab}$ is the total energy per unit cell of the zirconium slab with a clean surface, and the reference energy $E_{total}^{oxygen\ atom}$ is the total energy of the oxygen atom calculated with a pseudopotential. From Figs. 2(a) and 2(b), we see that for both the (2×1) and (1×1) systems the octahedral sites O(23) between the second and third layer are the most stable sites. It has been the conclusion of some experiments that the oxygen atoms occupy the subsurface octahedral site O(12) in the initial oxygen process of Zr.[5–10] Our results support subsurface adsorption models. However, the most favorable adsorption sites are found to be between *the second and the third layer*, rather than between the top and the second layer. Our calculations show that the adsorption energy of the O(23) sites is lower than the O(12) sites by almost 0.4 eV. It is thus rather unlikely that the O(12) sites can compete with O(23) sites. The O(12) sites are actually less favorable than the overlayer adsorption sites. For example, the surface fcc site has lower energy than the O(12) site by about 0.18 eV for the (2×1) and about 0.28 eV for the (1×1) structure.

The overlayer fcc site is slightly more favorable than the overlayer hcp site by about 0.24 eV for the (2×1) and about 0.18 eV for the (1×1) structure. If the oxygen atoms penetrate the Zr top layer, the high symmetry sites are the octahedral and the tetrahedral interstitial sites in the Zr host. From Figs. 2(a) and 2(b), we see that the subsurface tetrahedral sites are always less stable compared with the octahedral sites. This is in agreement with the LEED structure analysis.[5,10] From Fig. 1(a), we can easily see that the surface fcc sites can be regarded as the continuation of the subsurface octahedral sites, while the hcp sites are directly above the one kind of the tetrahedral sites. We already see that the surface hcp sites are slightly less favorable. In the subsurface configurations, the interstitial vacancy of the tetrahedral sites has a much smaller geometrical volume compared with that of the octahedral sites. This will lead to large strain and mandates a large relaxation of the host lattice, as we will see in a later section. This probably contributes the higher energy at the tetrahedral sites.

If we compare the binding energies at the O(23) sites for the two different coverages, we find that the binding energies of oxygen are -9.1 eV and -10.0 eV for the (1×1) system and the (2×1) system, respectively. The binding energy is thus stronger at the lower coverage. The binding at the subsurface sites for the (1×1) system is more stable than the calculated binding energy of cubic, tetragonal, and monoclinic zirconium-dioxide (zirconia), which are -8.83, -8.85, and -8.87 eV, respectively (using bulk Zr and
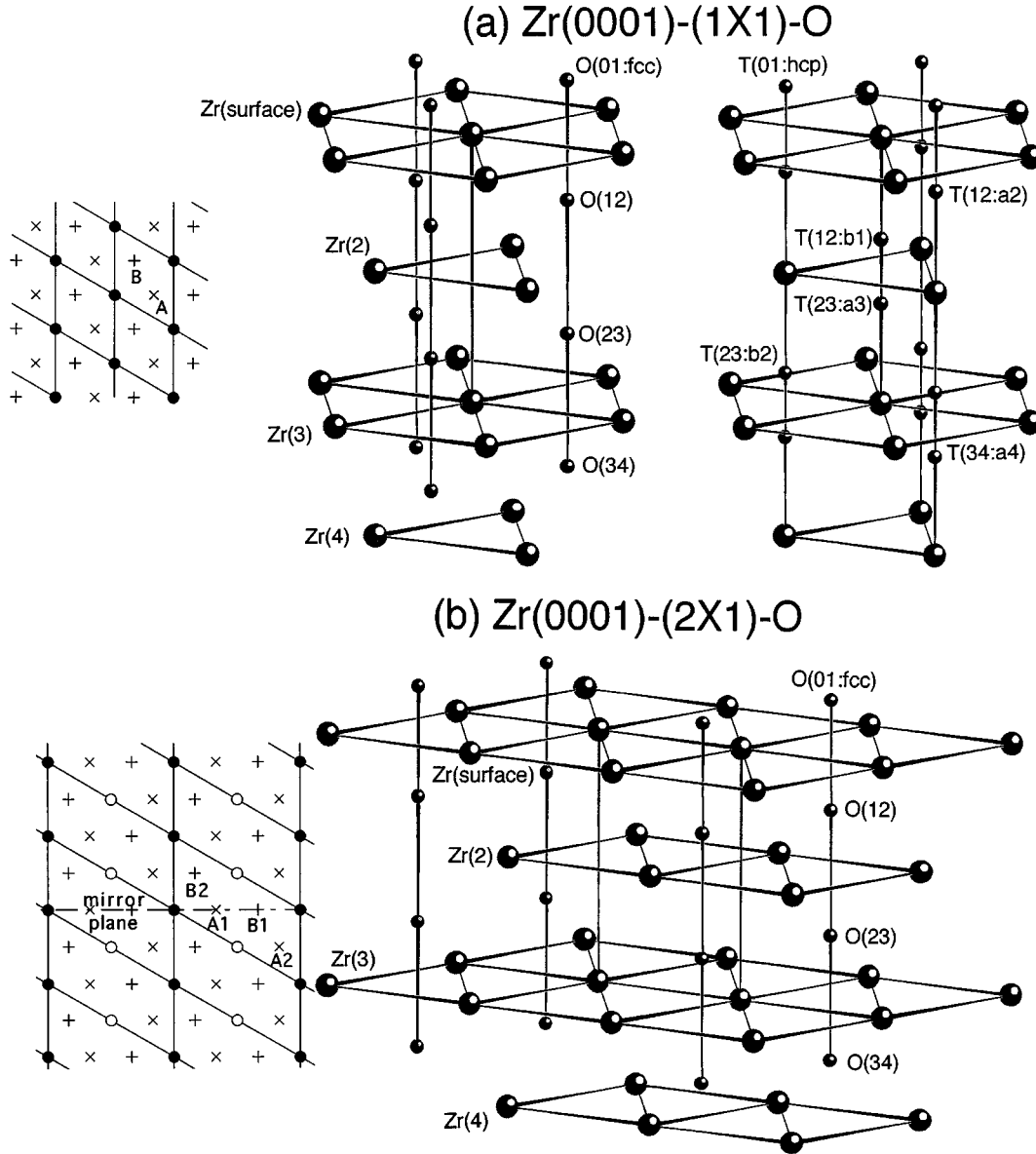
(a) Zr(0001)-(1X1)-O

(b) Zr(0001)-(2X1)-O

FIG. 1. Oxygen adsorption sites for (a) the (1×1) structure and (b) the (2×1) structure. Here O(xy) means the octahedral site between the xth and the yth metal layer. $T[xy:a$ (or $b)z]$ means the tetrahedral site located above (or below) the zth metal layer and between the xth and the yth metal layer. In the (2×1) structure, the T sites are not shown.

atomic oxygen as reference).[25] Basing on these results on the (0001) surface, it is reasonable to expect that the formation of a chemisorbed layer of the oxygen structure at subsurface sites precedes the surface oxide growth.

The adsorption energy is defined as the energy per oxygen atom gained by the adsorption of the oxygen molecule onto the relaxed Zr(0001)-(1×1) clean surface:

$$E_{ad}(\Theta) = [E_{total}^{slab}(\Theta) - E_{total}^{Zr\ slab}]/N_{oxygen} - [2E_{total}^{oxygen\ atom} - D]/2$$

$$= E_b(\Theta) + D/2. \qquad (2)$$

We have used the experimental value of 5.116 eV for the dissociation energy D of oxygen. The results are shown in Table I. To the best of our knowledge, the adsorption energy of oxygen on Zr(0001) has not been determined experimentally. The heat of absorption, which is defined as the energy

difference between the oxygen in the zirconium bulk and the gas state, has been reported to be -6.42 to -5.85 eV per O atom in the α phase of zirconium,[28] where oxygen atoms are dissolved at octahedral sites in hcp zirconium metal. In our calculation of the heat of oxygen absorption of Zr_2O with anti-CdI$_2$ structure is -6.78 eV per atom,[25] which is in agreement with the above experimental value, allowing for the fact the LDA usually overbinds.

The calculated adsorption energy at the O(23) subsurface site for the (2×1) system is substantially more favorable (0.67 eV) than the bulk heat of absorption, while the adsorption energy for the higher coverage (1×1) system is less stable (by 0.21 eV) than the bulk heat of absorption. This may be due to the oxygen-oxygen interaction. To carry out a rough estimate of the interaction energy between the adatoms we write the chemical potential of the adsorption system
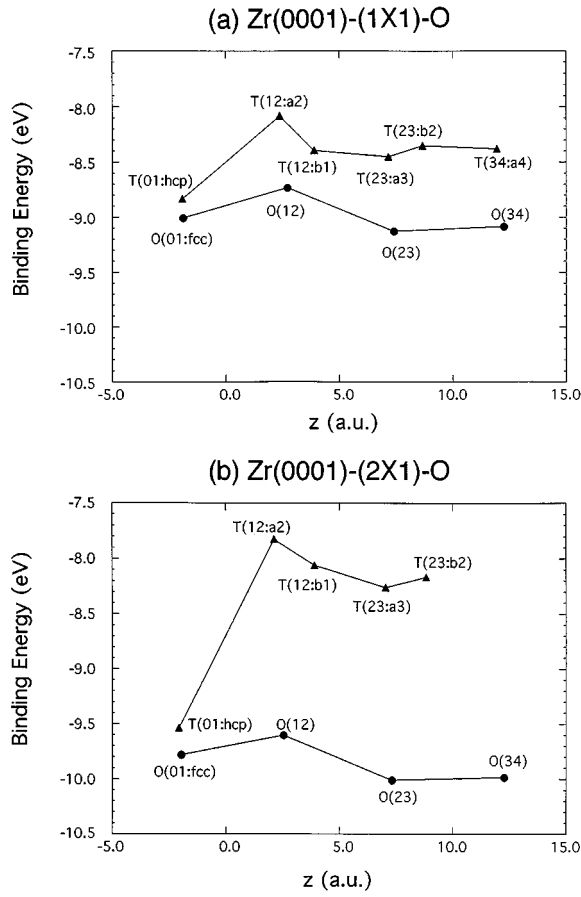
FIG. 2. Binding energies of oxygen for (a) the (1×1) structure and (b) the (2×1) structure as a function of the distance from the surface.

$$\mu = \frac{\partial [N_{\text{oxygen}} E_{ad}(\Theta)]}{\partial N_{\text{oxygen}}} = E_{ad}(\Theta) + \Theta \frac{\partial E_{ad}(\Theta)}{\partial \Theta}. \quad (3)$$

In the mean field theory the chemical potential at zero temperature is given by[29]

$$\mu = E_{ad} - 2z \epsilon_{\text{pair}} \Theta, \quad (4)$$

where z is the coordination number of adatoms and $-2\epsilon_{\text{pair}}$ is the pair interaction energy between the adatoms.

The positive ϵ means the interaction is attractive. From the above two equations the $\partial E_{ad}(\Theta)/\partial \Theta$ gives the interaction energy $-2z \epsilon_{\text{pair}}$. The calculated values of the derivative are shown in Table I. Here we assume the derivative at the half monolayer (ML) is given by the difference of the adsorption energies at $\Theta = 0.5$ and $\Theta = 1$. The interaction at the fcc, hcp, and the octahedral sites below the surface are repulsive and the interaction energies have almost the same magnitude. If we assume $z = 6$, there is a strong repulsive interaction energy 0.24–0.30 eV per pair in the half ML system. The $\partial E_{ad}(\Theta)/\partial \Theta$ at the tetrahedral sites under the surface have negative values. The large interaction at a small distance between the adatom and the neighboring zirconium atoms may be the origin.

B. Relaxation

In Table II, the multilayer relaxation of the zirconium slab in the [0001] direction is shown for some adsorption structures. The relaxation Δ_{ij} is defined as the change of the interlayer distance between the ith and the jth zirconium layers, where the position of the zirconium layer is averaged over the two atomic position on the same (0001) plane in the case of (2×1) structure. The distances $r_{\text{Zr-O}}^{\text{min}}$ and $z_{\text{Zr-O}}^{\text{min}}$ are the nearest-neighbor zirconium-oxygen distance and the nearest-neighbor zirconium-oxygen interlayer distances, respectively.

In the oxygen adsorption at the overlayer fcc and hcp sites the Δ_{12} is positive (expansion) for the (1×1) system, but negative (contraction) for the (2×1) system. When oxygen atoms adsorb at the underlayer octahedral sites, the relaxations between the zirconium interlayers which sandwich the oxygen layer are more than 10% for the (1×1) system and less than 10% for the (2×1) system, and the relaxations are increased at the deeper layer absorption sites. The relaxation between the layers that sandwich the tetrahedral oxygen site is approximately 30% for both the (1×1) and (2×1) systems. Such a large relaxation may be one of the origin that the adsorption of oxygen at the octahedral sites is more favorable than that at the tetrahedral site.

The relaxation Δ_{12} becomes close to the clean surface value -4.7% (Ref. 20) when the oxygen atoms adsorb at the deeper absorption site. This may be related to the fact that the metallic character at the surface is recovered for the

TABLE I. Calculated binding energy, adsorption energy, and differential adsorption energy per oxygen atom.

Adsorption Site	Zr(0001)-(2×1)-O, $\Theta = 1/2$			Zr(0001)-(1×1)-O, $\Theta = 1$	
	E_b (eV)	E_{ad} (eV)	$\partial E_{ad}/\partial \Theta$ (eV)	E_b (eV)	E_{ad} (eV)
O(01:fcc)	−9.78	−7.22	1.55	−9.01	−6.45
O(12)	−9.60	−7.04	1.74	−8.73	−6.17
O(23)	−10.01	−7.45	1.76	−9.13	−6.57
O(34)	−9.98	−7.43	1.80	−9.08	−6.53
T(01:hcp)	−9.54	−6.98	1.41	−8.83	−6.27
T(12:$a2$)	−7.83	−5.27	−0.51	−8.08	−5.52
T(12:$b1$)	−8.06	−5.50	−0.66	−8.39	−5.76
T(23:$a3$)	−8.26	−5.70	−0.38	−8.45	−5.89
T(23:$b2$)	—	—	—	−8.35	−5.79
T(34:$a4$)	—	—	—	−8.38	−5.82

TABLE II. Relaxation of the zirconium interlayer spacings and the nearest-neighbor zirconium-oxygen distances.

	Relaxation (%)					Distance (a.u.)	
	Δ_{12}	Δ_{23}	Δ_{34}	Δ_{45}	Δ_{56}	$r_{Zr\text{-}O}^{min}$	$z_{Zr\text{-}O}^{min}$
Zr(0001)(10 layers)[a]	−4.7	+1.2	+1.0	−0.6	+0.3		
Zr(0001)(8 layers)[a]	−4.4	+1.0	+1.0	−0.8			
Experiment[b]	−1±2						
Experiment[c]	−1.6±0.8	+0.4±1.2	0.0±1.2	0.0±1.6			
(1×1)-O(01:fcc)	+2.5	−1.8	−1.3	+0.6	±0.0	3.95	1.88
(1×1)-T(01:hcp)	+3.4	−2.4	−1.3	+0.6	−0.3	3.97	1.92
(1×1)-O(12)	+10.9	−1.5	+0.9	−0.7	±0.0	4.36	2.64
(1×1)-O(23)	−2.9	+11.4	+0.1	+0.6	+0.7	4.40	2.69
(1×1)-O(34)	−3.9	+0.1	+12.2	−1.6	−0.1	4.39	2.68
(1×1)-T(12:a2)	+30.1	−0.8	−2.4	−0.3	−0.9	3.92	3.92
(1×1)-T(12:b1)	+30.1	−0.6	−2.2	−0.7	−1.0	3.90	3.90
(1×1)-T(23:a3)	−2.8	+32.1	−1.3	−2.2	−0.4	3.94	3.94
(1×1)-T(23:b2)	−2.7	+31.5	−0.5	−1.6	−1.8	3.96	3.96
(1×1)-T(34:a4)	−4.2	+0.7	+30.8	+0.3	−4.1	3.92	3.92
(1×1)-Experiment[d]						4.35	2.55
(1×1)-Experiment[c]	+3.1	+2.3	+0.4	0.0		4.31	2.48
(2×1)-O(01:fcc)	−2.3	−0.4	±0.0	−0.2	—	3.95	1.87
(2×1)-T(01:hcp)	−1.9	−0.8	−0.4	+0.1	—	4.00	1.97
(2×1)-O(12)	+2.9	+0.2	+2.8	+6.2	—	4.23	2.42
(2×1)-O(23)	−2.6	+7.6	+1.4	+2.1	—	4.33	2.58
(2×1)-O(34)	−3.5	+2.5	+8.3	+2.3	—	4.34	2.61
(2×1)-T(12:a2)	+25.7	+0.7	−1.6	−1.1	—	3.90	3.90
(2×2)-Experiment[e]						4.37	2.59
(2×2)-Experiment[f]	+2.3	+1.6	−0.8	0.0		4.23	2.46

[a]Reference 20.
[b]Reference 30.
[c]Reference 16.
[d]Reference 10.
[e]Reference 5.
[f]Reference 15.

deeper site adsorption, which can be seen from the charge density and the electronic structure described below. Since the accommodation required for the adsorbed oxygen per layer in the (2×1) system is less than that in the (1×1) system, the relaxation Δ_{ij} of the (2×1) system is generally smaller than that of the (1×1) system. The interatomic distances $r_{Zr\text{-}O}^{min}$ and the interlayer distances $z_{Zr\text{-}O}^{min}$ are in agreement with the experimental results determined by LEED structure analysis.[5,10,15,16] The interatomic distances $r_{Zr\text{-}O}^{min}$ at the overlayer fcc and hcp sites are shorter than those at the underlayer octahedral sites and almost the same as those at the underlayer tetrahedral sites. This is in good agreement with the LEED structure analysis.[10] The interatomic distance $r_{Zr\text{-}O}$ is 4.29–4.39 a.u. in the solid solution α phase, and 3.86–4.27 a.u. in the zirconium oxide ZrO_2 phase. Our calculated interatomic distances $r_{Zr\text{-}O}^{min}$ for oxygen in the interior sites are in good agreement with those in the solid solution α phase. The displacements of the atomic position of the octahedral site from the center of the two sandwiching layers are less than 1%, but for the tetrahedral site the atomic positions are displaced more than 10% from the ideal

tetrahedral-site position. This may be closely related to the large interlayer relaxation, which deforms the tetrahedron from its ideal shape.

Since the (2×1) structure has a lower symmetry than the (1×1) structure, the structural relaxation has additional degrees of freedom: corrugation of the Zr (0001) planes and the lateral displacements in the $[10\bar{1}0]$ direction on the mirror plane. We found that the corrugation is typically 3% to 4% of the ideal Zr interlayer spacing. The atomic displacements on the mirror plane are less than 1% of the zirconium interatomic distance on the (0001) plane. The lateral displacement obtained by the TLEED structure analysis for the (2×2) structure is 5.9%,[15] which is greater than our value. This may be due to the more open structure in the lateral direction for the (2×2) structure than for the (2×1) structure.

C. Work function

In Figs. 3(a) and 3(b), the work function changes ($\Delta \phi$) in comparison to the clean Zr(0001) surface are shown for the
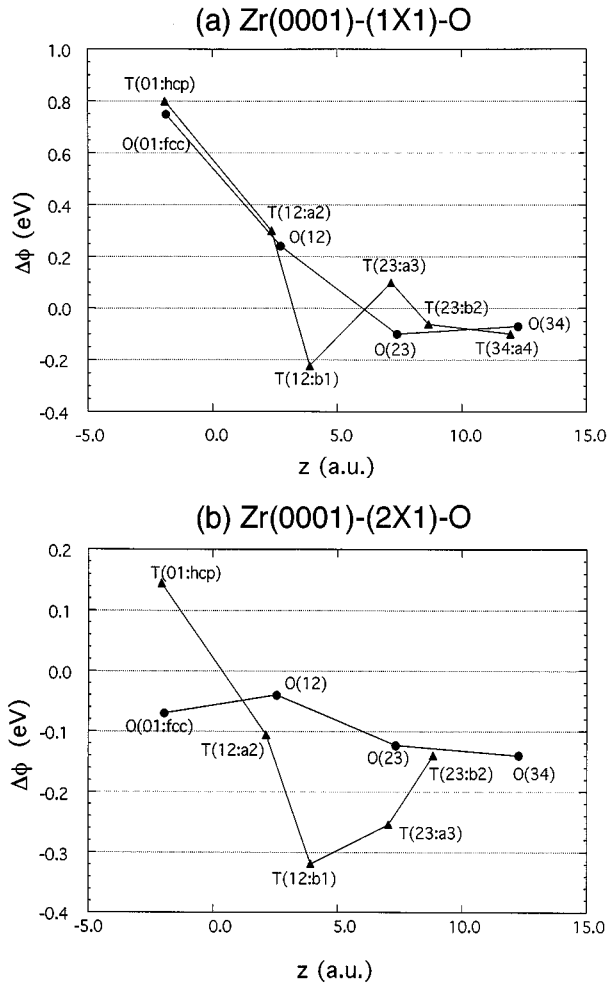
FIG. 3. Change in the work function by oxygen adsorption for (a) the (1×1) structure and (b) the (2×1) structure in comparison with that of the clean Zr(0001) surface, which is shown as a function of the distance from the surface.
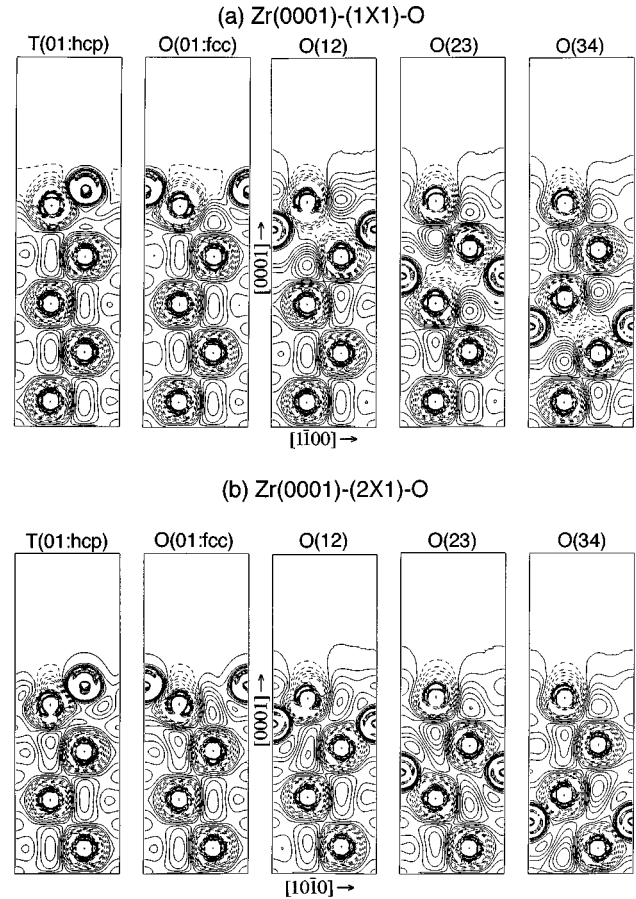

FIG. 4. Charge distribution difference between the self-consistent (pseudo)charge density for the slab and the superposition of (pseudo)atomic charge density for (a) the (1×1) structure and (b) the (2×1) structure. Solid and dashed contours correspond to the regions of charge accumulation and depletion, respectively. The planes spanned by the vectors $[1\bar{1}00]$ and $(1/2)[0001]$ are shown for the (1×1) structure and the planes spanned by the vectors $[10\bar{1}0]$ and $(1/2)[0001]$ are shown for the (2×1) structure. Charge densities on successive contours differ by 0.002 electrons/(a.u.)^3.

(1×1) and (2×1) structures, respectively. We have used the work functions of the clean surface, which were calculated to be 4.26 and 4.37 eV for the slab with eight and ten zirconium layers, respectively.[20] It is generally believed that the work functions increase (decrease) when the negatively charged adatom such as oxygen adsorbs above (below) the surface.[31] Intuitively, we expect that charge is transferred from the Zr atoms to the more electronegative oxygen atoms, and if the oxygen atoms are above the surface, the surface dipole will tend to increase the work function, whereas if the oxygen atoms are just below the surface, the dipole points to the opposite direction and decreases the work function. The change in $\Delta \phi$ should diminish as the oxygen atoms are buried deeper into the bulk and screened by the Zr conduction electrons. The general trend of our results, as shown in Figs. 3(a) and 3(b), is consistent with this picture: $\Delta \phi$ generally goes from positive to negative when the oxygen layer penetrates the Zr surface. However, we should point out such a simplified model basing on electronegativity and surface dipole arguments does not always prevail. For example, it cannot account for simple adsorption systems such as alkali-metal adsorption on jellium surface.[32] A more careful examination of Fig. 3 shows that the work function change is

very sensitive to the position of the oxygen adatom. For example, the overlayer adsorption at the (2×1)-O(01:fcc) site decreases the work function slightly by 70 meV, while the overlayer adsorption at the (2×1)-T(01:hcp) site increases the work function by 150 meV. The adsorption at the subsurface sites O(12) and T(12:a2) and the inner T(23:a3) site in the (1×1) structure increases the work function by 300, 260, and 100 meV, respectively.

The work function change has been measured carefully,[7,8] and the sensitivity of $\Delta \phi$ to the position of the oxygen atoms can help us identify the adsorption site. Experimentally, the work function is found to decrease initially with coverage, reaching a minimum at about a half monolayer (ML) coverage.[8] The experimentally found decrease in work function is certainly consistent with the subsurface site for the oxygen atoms. It also indicates that the oxygen cannot be very far from the surface because both intuition and our theoretical results indicate that $\Delta \phi$ should be small if the oxygen adatoms are deeply buried. From the calculated large positive $\Delta \phi$ for the (1×1) system the overlayer O(01:fcc) and the subsurface O(12) adsorption of oxygen may be excluded

in comparison with the experimental results. The $\Delta\phi$ of the oxygen adsorption at the energetically most favorable O(23) site is -80 and -120 meV for the (1×1) and the (2×1) systems, respectively. Zhang *et al.* have measured $\Delta\phi$ for the zirconium(0001) surface oxidized at room temperature and followed by a brief annealing at 493 K, which resulted in the formation of the ordered phase of oxygen adatoms, and found that $\Delta\phi$ is -320 and -290 meV at a half ML and one ML coverage, respectively.[8] It is rather satisfying that the energetically most favorable sites for (1×1) and (2×1) give negative $\Delta\phi$, and the (2×1) work function is lower than the (1×1) work function, in accordance with experimental findings. On the other hand, we note that the experimental results are lower than our value by approximately 200 meV. There are two possible explanations for this difference. First, previous experience shows that LDA calculated work functions are typically good to about 0.1 to 0.2 eV, and there is no reason to expect a better agreement for this particular system. In addition, the work function is determined by comparing the vacuum level with the Fermi level in the calculation, and the numerical results are inevitably dependent on the thickness of the vacuum and the number of layers in the slab. Since these parameters are primarily chosen for structural and energetics considerations, there may still be room for improvement when we consider work functions. We found that the work function is decreased from 4.36 to 4.27 eV by changing the number of layers in the slab[20] and there is a 0.2 eV overestimation in comparison with the experimental value of 4.05 eV.[33] The second reason is hydrogen adsorption[4] and its segregation on the zirconium(0001) surface below 467 K.[34] The presence of the hydrogen on the surface increases the $\Delta\phi$ by more than $+150$ meV compared to the clean surface. Hydrogen contamination is almost impossible to remove from the group IV transition metal surfaces.[4]

D. Charge density and interlayer force field

The change in the electron density is shown for some configurations of the (1×1) and (2×1) structure in Figs. 4(a) and 4(b). The change $\Delta\rho$ is defined by the difference of the total charge and the superposition of atomic charge density:

$$\Delta\rho(\mathbf{r}) = \rho^{slab}(\mathbf{r}) - \sum_{l,j} \rho_j^{atom}(\mathbf{r} - \mathbf{R}_l - \mathbf{r}_j). \quad (5)$$

Here ρ^{slab} is the self-consistent (pseudo)charge density of the slab with adsorbed oxygen atoms, and $\rho_j^{atom}(\mathbf{r} - \mathbf{R}_l - \mathbf{r}_j)$ is the (pseudo)atomic charge density of the jth atom in the unit cell l. We found that the effect of the oxygen adsorption on the charge redistribution is mostly local, in the sense that only the nearest-neighbor regions are affected. A rough estimate of the accumulation of the electron charge around oxygen has been done by integrating $\Delta\rho(r)$. Surprisingly the electron accumulation around the oxygen atom (as found from $\int \Delta\rho d\mathbf{r}$) has almost the same value $0.4e$ within the 2.0–2.2 a.u. radius for all the sites both in the (1×1) and (2×1) structures. The excess charge of $0.4e$ is much smaller than that of the O^{2-} ion, which is consistent with the well known fact that directional covalent bonds contribute substantially to the zirconium-oxygen interaction in zirconium dioxide (zirconia).[25,35] Our calculation of the electronic charge accumulation for the oxygen in the cubic zirconia is about $0.7e$.[25] The charge accumulation around oxygen adatoms in the slab is thus lower than that in the oxide, and may suggest a more covalent nature of zirconium-oxygen interaction in this adsorption system.

We have also calculated the interlayer force fields, and found that they are fairly short ranged. The magnitude of interlayer force constants between the oxygen layer and the next-nearest-neighbor zirconium layer is approximately one-tenth of that of the force constants between the oxygen layer and the nearest-neighbor layer. Here the interlayer force constants are obtained by applying a small displacement of the oxygen layer in the [0001] direction from the fully relaxed position. Using the interlayer force constants we have calculated the oxygen vibrational energy in the [0001] direction for the (1×1) structure. The vibrational energies are 67, 61, and 58 meV for the oxygen adsorbed at the sites O(01:fcc), O(12), and O(23), respectively. We are not aware of experimentally measured frequencies, but these values compare well with the vibrational energy of 65 meV for Ti(0001)-oxygen adsorption measured by high resolution electron energy loss spectroscopy.[4]
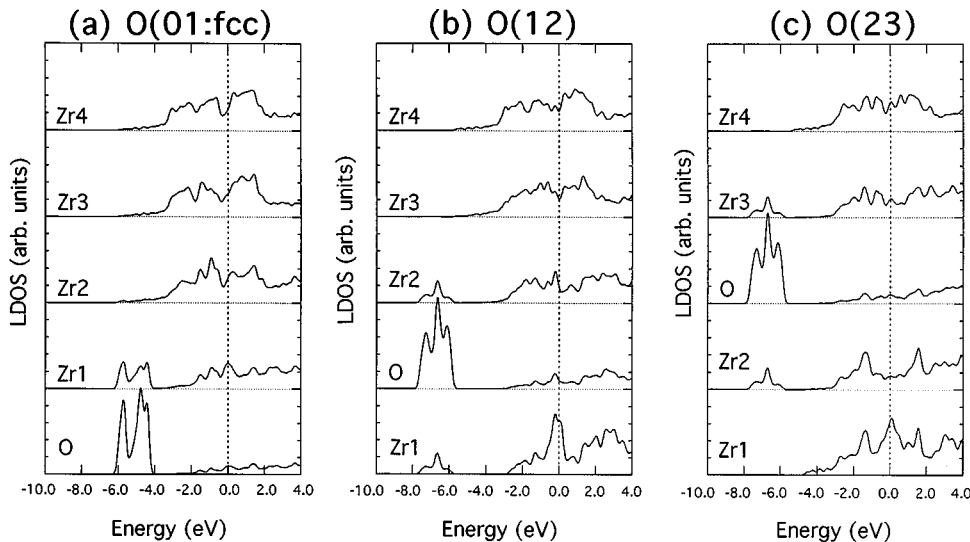

FIG. 5. Local density of states (LDOS) of the Zr(0001)-(1×1)-O structure for (a) the O(01:fcc) site adsorption, (b) the O(12) site adsorption, and (c) the O(23) site adsorption. The zero energy corresponds to the Fermi level.

E. Electronic structure

The layer-decomposed local density of states (LDOS) for the (1×1) structure is evaluated using the following definition:

$$D(i,E) \equiv \sum_{\mathbf{k}_\parallel,n} \int_{(z_{i-1}+z_i)/2}^{(z_i+z_{i+1})/2} \rho_n^{\mathrm{sym}}(\mathbf{k}_\parallel,z)\delta[E-E_n(\mathbf{k}_\parallel)]dz. \tag{6}$$

Here, $\mathbf{k}_\parallel$ is a wave vector in the two-dimensional Brillouin zone, n is a band index, z_i is the z position of the ith layer, and $\rho_n^{\mathrm{sym}}(\mathbf{k}_\parallel,z)$ is the layer-averaged charge density symmetrized from the probability density of the wave functions of the state $E_n(\mathbf{k}_\parallel)$ in the irreducible Brillouin zone.[24] $\rho_n^{\mathrm{sym}}(\mathbf{k}_\parallel,z)$ is normalized to unity in the unit cell. The summation of $\mathbf{k}_\parallel$ was done over 66 evenly spaced $\mathbf{k}$ points in the two-dimensional irreducible Brillouin zone, and 112 bands were considered. The δ-function in the above equation is replaced by a Gaussian function with 0.15 eV width.

In Figs. 5(a), 5(b), and 5(c), the local density of states (LDOS) of the (1×1) system for the O(01:fcc), O(12), and O(23) sites is shown. The Fermi energy is set at 0 eV. Although the oxygen-zirconium interaction is strong, the oxygen-induced change in the Zr LDOS is short-ranged, and is conspicuous only in the metal layers sandwiching the oxygen atoms.

The most prominent feature in the LDOS is the oxygen $2p$ band and the corresponding bonding band of Zr. The energies of the LDOS of this oxygen band for the O(12) and O(23) sites are shifted downward by about 1.6 eV from that of the overlayer O(01:fcc) site, indicating a stronger interaction between oxygen and zirconium when the oxygen is subsurface, probably due to an increase in the coordination number. The bandwidth of the oxygen $2p$ band is approximately 2 eV for the three oxygen sites. The bandwidth depends mainly on the oxygen-oxygen interaction and is approximately the same for the same coverage.

Surface states with high LDOS near the Fermi level are found for the underlayer oxygen adsorption. Surface states with high LDOS around the Fermi level have been found for zirconium and titanium clean (0001) surfaces.[20,36] These states are the most "reactive" and are removed upon interaction with oxygen atoms when the oxygen atoms adsorb outside the Zr surface. However, these surface states are quickly recovered when the oxygen atoms go subsurface. We can also observe this recovering from the charge difference contour plots in Fig. 4. The contours of the charge distribution differences at the surface layer are almost the same for underlayer oxygen adsorption at the O(12), O(23), and O(34) sites. This is a manifestation of the strong screening power of the metal conduction electrons. For the clean Zr surface, the high LDOS of the surface Zr layer near the Fermi level contributes to the surface energy. Upon oxidation, these surface states interact with the oxygen and are quenched. It is interesting to note that for oxygen atoms between the surface and the second Zr layers, the oxygen-zirconium bonding is stronger but the surface states near the Fermi level recover, leading to higher band energy contribution from the top layer Zr atoms. The overall effect seems to favor the surface site over the O(12) site.
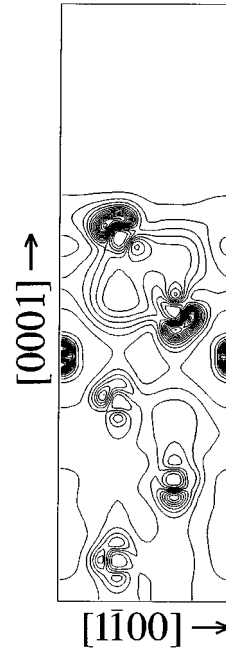

FIG. 6. Pseudocharge distribution contours of the states with energies between -1.6 eV and -1.1 eV for the O(23) site adsorption with the Zr(0001)-(1×1)-O structure.

In the LDOS of the O(23) adsorption structure, there is also a high LDOS region in the surface and the second Zr layer, with energy at about -1.4 eV below the Fermi level. This high LDOS region is not found in the O(01:fcc) and the O(12) site adsorption systems. The charge density distribution for the states with the energy between -1.6 and -1.1 eV is shown in Fig. 6. From the contour plot, the states in this high LDOS region contribute to the (metallic) bonding between the Zr atoms in the first (surface) and the second layer. These surface states are probably pulled downward from near the Fermi level, and there is a possibility that these occupied bonding states may be one of the origin of the favorable oxygen adsorption at the O(23) site.

In Figs. 7(a) and 7(b), the band structures of the slabs with oxygen adsorbed at the O(23) sites are shown for both the (1×1) and the (2×1) systems along the high symmetry lines in the two-dimensional irreducible Brillouin zone. In these figures, the closed (open) circles indicate that the population of the wave function in the oxygen (zirconium surface) layer exceeds 40%.

The oxygen $2p$ bandwidth of 2.1 eV for the (1×1) structure is wider than the 1.1 eV of the (2×1) structure. The larger dispersion originates from the strong oxygen-oxygen interaction in the higher coverage (1×1) structure as mentioned before. The band centers of the oxygen $2p$ band are located at 6.8 eV below the Fermi level for both structures.

Within about 1 eV of the Fermi level, the dispersions of the surface states at the zirconium surface layer for the (1×1) structure are almost the same as the surface states and the resonances of the clean Zr(0001) surface.[20] These surface localized states have been found for all the underlayer oxygen adsorption in the (1×1) and (2×1) systems. Using photoemission measurements and a band structure calculation, Feibelman *et al.* have shown that the subsurface adsorptions of hydrogen and nitrogen on the Ti(0001) surface do not
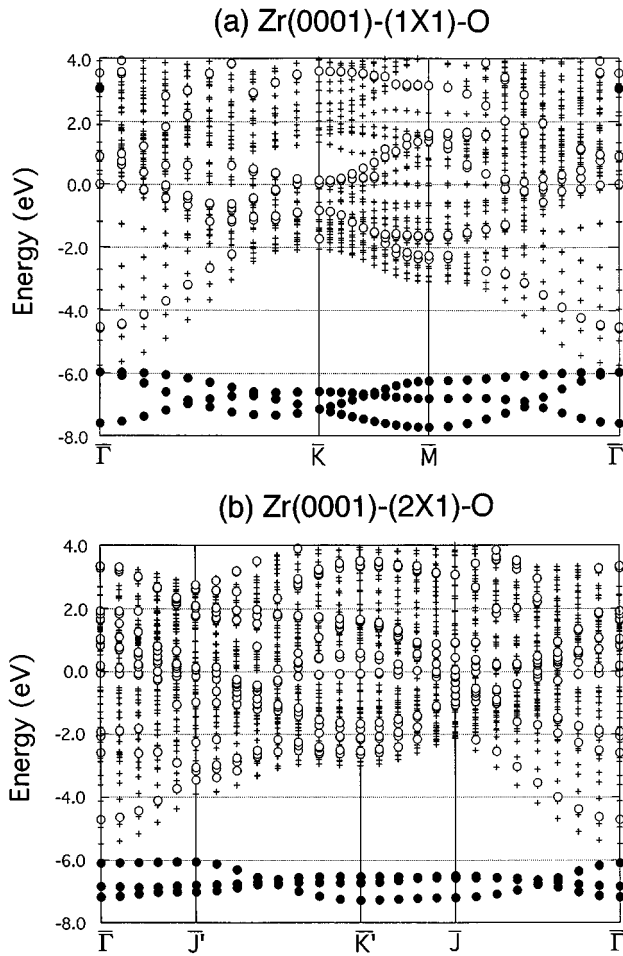
(a) Zr(0001)-(1X1)-O

(b) Zr(0001)-(2X1)-O

FIG. 7. Band structures for (a) the O(23) site adsorption with the Zr(0001)-(1×1)-O structure, and (b) the O(23) site adsorption with the Zr(0001)-(2×1)-O structure along high symmetry lines in the surface Brillouin zone. Open and closed circles correspond to the localized states at the zirconium first layer and the oxygen layer, respectively. The energy zero corresponds to the Fermi level.

affect the high LDOS at the surface metal layer, but hydrogen adsorption at the overlayer sites decreases the LDOS at the surface layer.[17] This universal ''short-range screening phenomenon''[17] is observed in the band structures for the oxygen adsorptions at the O(01:fcc), O(12), and O(23) sites in the (1×1) and (2×1) structures.

In Fig. 8, the charge densities of states localized at the oxygen layer and at the surface zirconium layer are shown for the oxygen adsorption at the O(23) site of the (1×1)-O structure for several energies at the $\bar{\Gamma}$ point. We found from the density contour that the oxygen $2p$ states with energy -7.6 eV below the Fermi level have p_z character and the states with energy -6.0 eV below the Fermi level have $p_{x,y}$ character. The surface state near the Fermi level has $d_{3z^2-r^2}$ character which has the same character as the surface state at the Fermi level of the clean Zr(0001) surface.[20]
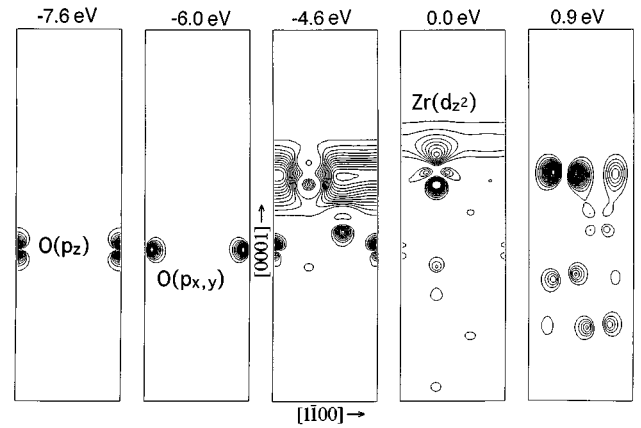

FIG. 8. Density contours of the $\bar{\Gamma}$ point wave functions localized at the oxygen layer and at the surface zirconium layer for the O(23) site adsorption with the Zr(0001)-(1×1)-O structure. The plane spanned by the vectors $[1\bar{1}00]$ and $(1/2)[0001]$ is shown.

Angle resolved, polarization-dependent photoemission measurements for the underlayer adsorption of the Ti(0001)-(1×1)-N system have shown that the surface state at the Fermi level has Λ_1 symmetry (i.e., s, p_z, and $d_{3z^2-r^2}$). This is in agreement with our result.

In summary, we have used the first-principles calculations to study the structural and electronic properties of the the O/Zr(0001) system. The calculations in the single-layer adsorption model have shown that the octahedral adsorption site between the second and third metal layer is the most energetically favorable site for both of the (1×1) and (2×1) structures. Our calculations indicate a decrease in work function when the oxygen atoms are in the lowest energy sites, which is consistent with experimental measurements. Subsurface adsorption is not so uncommon, but stable adsorption sites between the second and the third layer is rather intriguing. The adsorption is found to be strongly exothermic and the oxygen atoms at subsurface adsorption sites are energetically more favorable than those in bulk oxides, indicating that the subsurface sites are stable against further migration into the bulk in the initial oxidation process. In the current studies, the oxygen atoms are confined to one layer. In the next step, we will also consider the energetics when the oxygen atoms are distributed in more than one layer.

[1] H. D. Shih and F. Jona, Surf. Sci. **60**, 445 (1976).

[2] B. T. Jonker, J. F. Morar, and R. L. Park, Phys. Rev. B **24**, 2951 (1981)

[3] R. L. Strong and J. L. Erskine, J. Vac. Sci. Technol. A **3**, 1428 (1985).

[4] S. J. Garrett, R. G. Egdell, and J. C. Rivière, J. Electron Spectrosc. Relat. Phenom. **54/55**, 1065 (1990).

[5] K. C. Hui, R. H. Milne, K. A. R. Mitchell, W. T. Moore, and M. Y. Zhou, Solid State Commun. **56**, 83 (1985).

[6] P. C. Wong and K. A. R. Mitchell, Can. J. Phys. **65**, 464 (1987).

[7] K. Griffiths, J. Vac. Sci. Technol. A **6**, 210 (1988).

[8] C.-S. Zhang, B. J. Flinn, I. V. Mitchell, and P. R. Norton, Surf. Sci. **245**, 373 (1991).

[9] B. J. Flinn, C.-S. Zhang, and P. R. Norton, Phys. Rev. B **47**, 16 499 (1993).

[10] P.C. Wong, K. C. Hui, B. K. Zhong, and K. A. R. Mitchell, Solid State Commun. **62**, 293 (1987).

[11] P. C. Wong and K. A. R. Mitchell, Surf. Sci. **187**, L599 (1987).

[12] P. C. Wong, J. R. Lou, and K. A. R. Mitchell, Surf. Sci. **206**, L913 (1988).

[13] C.-S. Zhang, B. Li, and P. R. Norton, Surf. Sci. **313**, 308 (1994).

[14] K. A. R. Mitchell (private communication).

[15] Y. M. Wang, Y. S. Li, and K. A. R. Mitchell, Surf. Sci. **342**, 272 (1995).

[16] Y. M. Wang, Y. S. Li, and K. A. R. Mitchell, Surf. Sci. **343**, L1167 (1995).

[17] P. J. Feibelman and F. J. Himpsel, Phys. Rev. B **21**, 1394 (1980).

[18] K. Shinjo, S. Onishi, M. Tsukada, and S. Sugano, J. Phys. C **14**, 5575 (1981).

[19] K. Shinjo and S. Sugano, Surf. Sci. **124**, 387 (1983).

[20] M. Yamamoto, C. T. Chan, and K. M. Ho, Phys. Rev. B **50**, 7932 (1994).

[21] M. Yamamoto, C. T. Chan, K. M. Ho, M. Kurahashi, and S. Naito, Phys. Rev. B **53**, 13 772 (1996).

[22] R. M. Dreizler and E. K. U. Gross, *Density Functional Theory* (Springer, Berlin, 1990).

[23] L. Hedin and B. I. Lundqvist, J. Phys. C **4**, 2064 (1971).

[24] C. Elsässer, N. Takeuchi, K. M. Ho, C. T. Chan, P. Braun, and M. Fähnle, J. Phys. Condens. Matter **2**, 4371 (1990).

[25] M. Yamamoto, S. Naito, C. T. Chan, and K. M. Ho (unpublished).

[26] K. M. Ho, C. Elsässer, C. T. Chan, and M. Fähnle, J. Phys. Condens. Matter **4**, 5189 (1992).

[27] C. T. Chan, K. P. Bohnen, and K. M. Ho, Phys. Rev. B **47**, 4771 (1993).

[28] *Gase und Kohlenstoff in Metallen*, edited by E. Fromm and E. Gebhardt (Springer, Berlin, 1976).

[29] M. C. Desjonquères and D. Spanjaard, *Concepts in Surface Physics* (Springer, Berlin, 1993).

[30] W. T. Moore, P. R. Watson, D. C. Frost, and K. A. R. Mitchell, J. Phys. C **12**, L887 (1987).

[31] J. Hölzl and F. K. Schulte, *Solid State Physics* (Springer, Berlin, 1979), pp. 1–150.

[32] H. Ishida, Phys. Rev. B **38**, 8006 (1988).

[33] D. E. Eastman, Phys. Rev. B **2**, 1 (1970).

[34] C. Zhang, B.J. Flinn, and P. R. Norton, J. Nucl. Mater. **199**, 231 (1993).

[35] E. V. Stefanovich, A. L. Shluger, and C. R. A. Catlow, Phys. Rev. B **49**, 11 560 (1994).

[36] P. J. Feibelman, J. A. Appelbaum, and D. R. Hamann, Phys. Rev. B **20**, 1433 (1979).